frontiers in Earth Science

ORIGINAL RESEARCH
published: 28 January 2022
doi: 10.3389/feart.2021.823319

Geochemical Characteristics and Origin of Tight Gas in Member Two of the Upper Triassic Xujiahe Formation in Western Sichuan Depression, Sichuan Basin, SW China

Xiaoqi Wu[1,2], *Quanyou Liu*[1,3]*, *Yingbin Chen*[1,2], *Jun Yang*[1,2], *Huasheng Zeng*[1,2] and *Huaji Li*[4]

[1]State Key Laboratory of Shale Oil and Gas Enrichment Mechanisms and Effective Development, Beijing, China, [2]Wuxi Research Institute of Petroleum Geology, Petroleum Exploration and Production Research Institute, Wuxi, China, [3]Petroleum Exploration and Production Research Institute, Beijing, China, [4]Exploration and Production Research Institute, Southwest Branch Company, Chengdu, China

Natural gas in the tight sandstone reservoirs in Member two of the Upper Triassic Xujiahe Formation in the Western Sichuan Depression of the Sichuan Basin has complex geochemical characteristics, and the origin and source of the tight gas are revealed based on the geochemical analysis and comparison in this study. The tight gas has the dryness coefficient of 0.950–0.994, which is positively correlated with the CH_4 content. The gaseous alkanes display positive carbon isotopic series, with the $\delta^{13}C_1$ and $\delta^{13}C_2$ values ranging from –35.6‰ to –30.3‰ and from –29.1‰ to –21.0‰, respectively, and the δD_1 values range from –176‰ to –155‰. Genetic identification based on the carbon and hydrogen isotopic compositions indicates that a small amount of tight gas is typically coal-derived gas, whereas most of the tight-gas samples have experienced mixing by oil-associated gas. Geochemical comparisons suggest that the tight gas displays distinct differences with the typical oil-associated gas in Member four of the Middle Triassic Leikoupo Formation in the Chuanxi gas field and the typical coal-derived gas in Member five of Xujiahe Formation in the Xinchang gas field. It is also apparently different from the typical coal-derived gas in Member two of Xujiahe Formation in both Zhongba and Qiongxi gas fields. Among the tight gas in Member two of the Xujiahe Formation from the Western Sichuan Depression, the coal-derived gas is generated mainly by the humic mudstone in the Upper Triassic Ma'antang and Xiaotangzi formations, with assistance of the humic mudstone in Member two of the Xujiahe Formation, whereas the oil-associated gas is derived from the sapropelic limestone in the Ma'antang Formation.

Keywords: tight gas, geochemical characteristics, genetic types, gas source, xujiahe formation

OPEN ACCESS

Edited by:
Deyu Gong,
Research Institute of Petroleum Exploration and Development (RIPED), China

Reviewed by:
Xiaofeng Wang,
Northwest University, China
Haifeng Gai,
Guangzhou Institute of Geochemistry (CAS), China

***Correspondence:**
Quanyou Liu
qyouliu@sohu.com

Specialty section:
This article was submitted to Geochemistry, a section of the journal Frontiers in Earth Science

Received: *27 November 2021*
Accepted: *24 December 2021*
Published: *28 January 2022*

Citation:
Wu X, Liu Q, Chen Y, Yang J, Zeng H and Li H (2022) Geochemical Characteristics and Origin of Tight Gas in Member Two of the Upper Triassic Xujiahe Formation in Western Sichuan Depression, Sichuan Basin, SW China. Front. Earth Sci. 9:823319. doi: 10.3389/feart.2021.823319

1 INTRODUCTION

Tight-gas reservoirs refer to the tight sandstone fields or traps which accumulate commercial natural gas, and they can be divided into continuous-type and trap-type (Dai et al., 2012a). As one important type of unconventional natural gas, tight gas has made a crucial contribution to the rapid increase of both the yields and reserves of natural gas in China. The proven reserves of tight gas in China reached

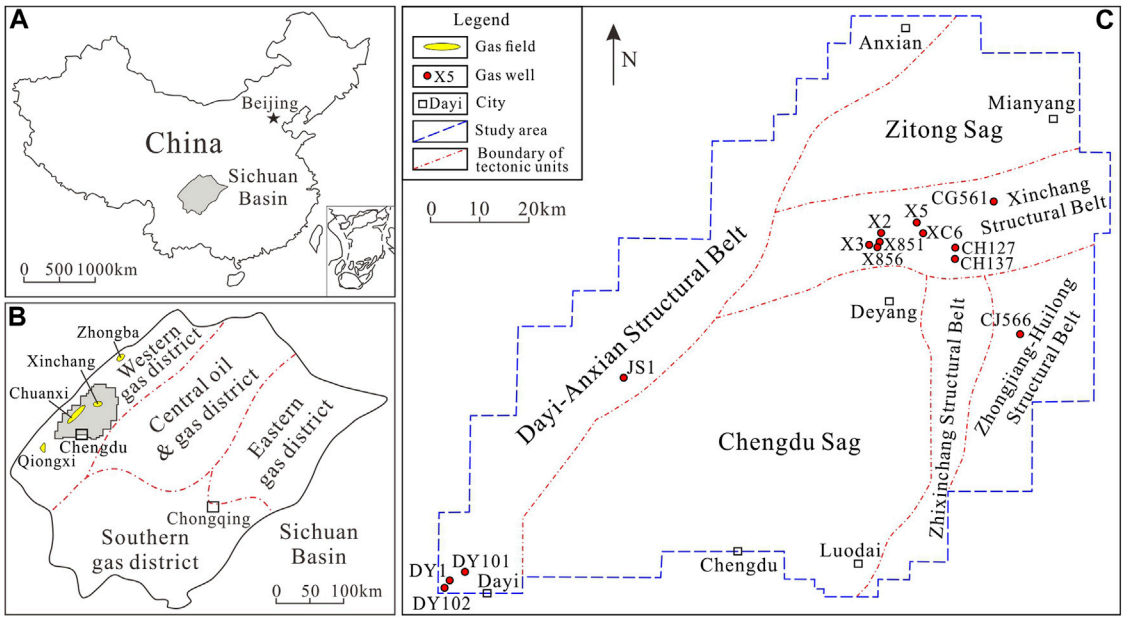

FIGURE 1 | The position of the Sichuan Basin in China **(A)**, the location of the depression in the Sichuan Basin **(B)**, and distribution of gas wells and structural units in the Western Sichuan Depression **(C)**.

3.0109×10^{12} m^3 by the end of 2010, which accounted for 39.2% of the total gas reserves (Dai et al., 2012a).

The Sichuan Basin is one of the important onshore petroliferous basins in China, and the exploration fields include terrigenous and marine strata (Dai et al., 2009; Dai et al., 2012b; Liu et al., 2012; Liu et al., 2013; Liu et al., 2014; Liu et al., 2016), with the former consisting of tight sandstone reservoirs in both the Upper Triassic Xujiahe Formation (T_3x) and Jurassic strata. The Zhongba gas field in Member two of the Xujiahe Formation (T_3x^2), located in the western Sichuan Basin, is the first tight-gas field discovered in China (Dai et al., 2014). Several giant tight-gas fields (e.g., Xinchang, Guang'an, Hechuan, and Anyue) with proven reserves exceeding 10×10^9 m^3 have been revealed during the gas exploration in the Xujiahe Formation of the Sichuan Basin (Dai et al., 2014).

The Western Sichuan Depression (WSD) is situated in the western Sichuan Basin, and the gas exploration has achieved successive breakthroughs in the Middle Triassic to Jurassic strata (Wu et al., 2017; Wu et al., 2020a; Wu et al., 2020b). The Member two of the Middle Triassic Xujiahe Formation (T_3x^2) has attracted wide attention due to the favorable exploration potential. The proven reserves of T_3x^2 in the Xinchang gas field from WSD are 121.12×10^9 m^3 (Dai, 2016), and the Zhongba and Qiongxi gas fields have also been discovered in the adjacent areas (Dai et al., 2012b).

The origin and source of tight gas in different strata of the Sichuan Basin have been extensively studied based on geochemical analysis, and the tight gas in the T_3x and Jurassic strata is considered as typical coal-derived gas and sourced mainly from the T_3x coal-measure source rocks (Dai et al., 2009; Dai et al., 2012b; Ni et al., 2014a; Ni et al., 2014b; Wu et al., 2017; Dai et al., 2018; Wu et al., 2019). The T_3x^2 gas from WSD displays complex geochemical characteristics, which are significantly different from the typical coal-derived gas from other members of T_3x. The authors intend to conduct geochemical analysis of the main components and stable carbon and hydrogen isotopes of the T_3x^2 gas from WSD, in order to reveal the genetic types and source of the gas as well as the differences with other reservoirs in the same area.

2 GEOLOGICAL SETTING

The Sichuan Basin is developed on the basis of the Upper Yangtze Craton in SW China (**Figure 1A**), covering an area of 180×10^3 km^2. It is the third largest petroliferous basin in China and superimposed by a marine craton and a terrigenous foreland basin. The annual gas yield in 2020 reaches 56.5×10^9 m^3, making it become the most productive petroliferous basin in China (Zhang, 2021). It consists of four exploration districts based on the structural units, i.e., Western, Eastern, and Southern gas districts, and Central oil and gas district (Dai et al., 2009).

The WSD is located in the central part of the Western gas district (**Figure 1B**), covering an area of 10×10^3 km^2. It is generally divided into four structural belts (Dayi-Anxian, Xinchang, Zhixinchang, and Zhongjiang-Huilong) and two sags (Zitong and Chengdu) (**Figure 1C**). The commercial gas wells in the Member two of the Xujiahe Fm. (T_3x^2) are mainly situated in the Xinchang and Dayi-Anxian Structural Belts (**Figure 1C**). The Qiongxi and Zhongba gas fields have been discovered in natural gas exploration to the southwest and north of WSD, respectively (**Figure 1B**).

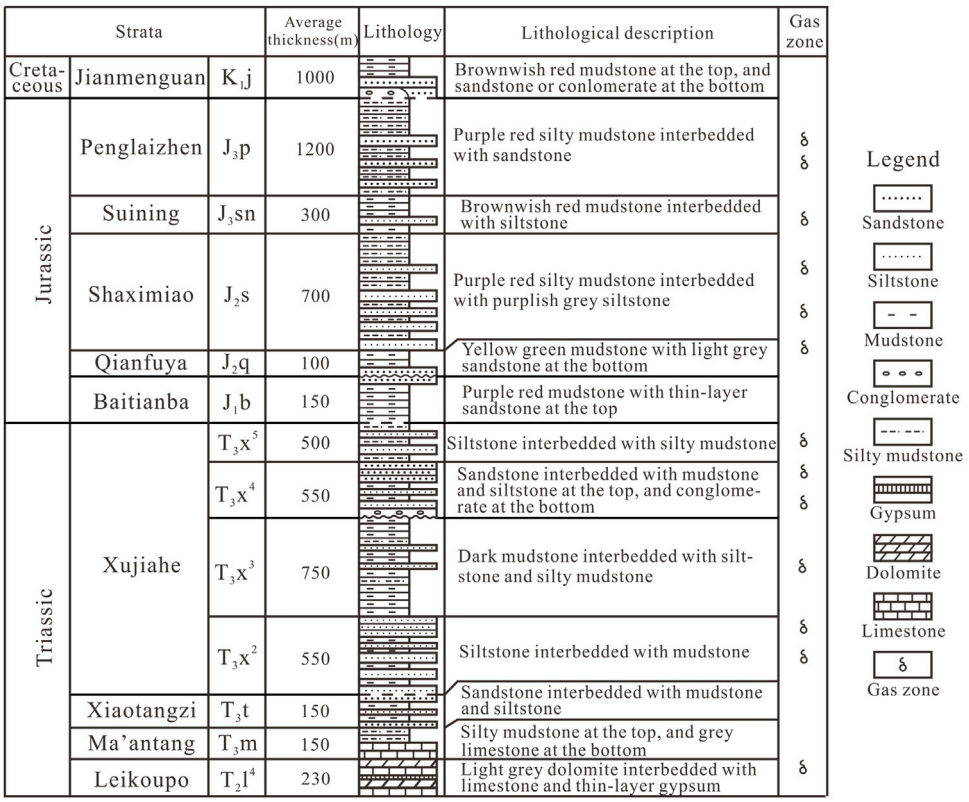

FIGURE 2 | Stratigraphic column of the Western Sichuan Depression, Sichuan Basin, China.

There are multiple gas-bearing layers in WSD, and the gas exploration has been conducted in Member four of the Middle Triassic Leikoupo Fm. (T_2l^4), Upper Triassic Xujiahe Fm. (T_3x), and Jurassic strata (**Figure 2**). The Xujiahe Fm. is commonly divided into six members bottom-up, i.e., Member 1 (T_3x^1) to Member 6 (T_3x^6), in which Member six is missing in the WSD due to weathering denudation, and Member one is generally divided into Xiaotangzi (T_3t) and Ma'antang (T_3m) formations (**Figure 2**). Member two of the Xujiahe Fm. (T_3x^2) consists of siltstone interbedded with mudstone, and it is conformably and disconformably contacted with the overlying Member three of T_3x and underlying T_3t, respectively.

3 SAMPLES AND ANALYTICAL METHODS

The T_3x^2 tight-gas samples in the WSD of the Sichuan Basin were collected from the wellheads using 5-cm-radius stainless steel cylinders with double valves, and the lines were flushed for 10–15 min in order to remove air contamination at first. A geochemical analysis of the gas samples was conducted at the Wuxi Research Institute of Petroleum Geology, Petroleum Exploration and Production Research Institute, SINOPEC.

The chemical composition of gas samples measured using an Agilent 7890A gas chromatograph (GC) equipped with a flame ionization detector and a thermal conductivity detector. Individual alkane gas components were separated using a capillary column (PLOT Al_2O_3 50 m × 0.53 mm × 25 μm). Helium was used as the carrier gas with a rate of 40 ml/min and unsplit stream sampling. The GC oven temperature was initially set at 40°C for 5 min, heating at a rate of 10°C/min to a final temperature of 180°C, which was held for 20 min.

The stable carbon isotopic composition of alkane gases was measured on a Finnigan MAT 253 mass spectrometer. The alkane gas components were initially separated using a fused silica capillary column (PLOT Q 30 m × 0.32 mm × 20 μm) with helium carrier gas at the flow rate of 10 ml/min. The gas was injected into the GC in the split injection model with the split ratio of 15:1. The oven temperature was ramped from 40°C to 180°C at a heating rate of 10°C/min, and the final temperature was held for 10 min. Each gas sample was measured in triplicate, and the results were averaged. Stable carbon isotopic values are reported in the δ notation in per mil (‰) relative to VPDB, and the measurement precision is estimated to be ±0.5‰ for $\delta^{13}C$.

The stable hydrogen isotopic composition of alkane gases was measured on a Thermo Scientific Delta V Advantage mass spectrometer (GC/TC/IRMS). The alkane gas components were separated on an HP-PLOT Q column (30 m × 0.32 mm × 20 μm) with helium carrier gas at 1.5 ml/min. The gas was injected into the GC in the split injection model with the split ratio of 15:1. The GC oven was initially held at 30°C for

TABLE 1 | Main components and stable carbon and hydrogen isotopic compositions of the T_3x^2 tight gas from the Western Sichuan Depression.

Tectonic units	Well	Components (%)						C_1/C_{1-4}	$\delta^{13}C$ (‰)			δD (‰)		
		CH_4	C_2H_6	C_3H_8	C_4H_{10}	N_2	CO_2		$\delta^{13}C_1$	$\delta^{13}C_2$	$\delta^{13}C_3$	δD_1	δD_2	δD_3
Dayi-Anxian Structural Belt	DY1	96.50	1.74	0.21	0.05	0.27	1.18	0.980	−32.0	−25.0	—	−160	—	—
	DY101	94.16	3.14	0.48	0.15	0.41	1.54	0.961	−31.8	−21.2	—	−163	—	—
	DY102	96.77	1.42	0.17	0.00	0.00	1.65	0.984	−32.7	−24.0	−24.9	−163	—	—
	JS1	96.68	0.51	0.04	0.04	0.69	1.94	0.994	−32.8	−25.3	−27.5	—	—	—
Xinchang Structural Belt	X2	97.28	0.83	0.07	0.02	0.23	1.53	0.991	−31.9	−28.3	—	−155	—	—
	X3	97.51	0.94	0.09	0.02	0.25	1.17	0.989	−31.4	—	—	−157	—	—
	X5	97.54	0.94	0.10	0.00	0.00	1.42	0.989	−31.6	−28.4	−28.2	−166	—	—
	X8-1H	97.27	0.80	0.08	0.00	0.55	1.28	0.991	−32.2	−26.7	−25.5	−159	−148	—
	X851	98.14	0.82	0.09	0.03	0.08	0.82	0.991	−30.3	−27.1	—	—	—	—
	X853	97.12	0.82	0.08	0.02	0.42	1.44	0.991	−31.2	−27.3	—	−159	—	—
	X856	97.45	0.81	0.07	0.02	0.63	0.94	0.991	−30.8	−29.1	−28.1	−157	−151	−115
	XC6	97.39	1.06	0.12	0.00	0.00	1.43	0.988	−31.9	−26.4	−26.8	−165	—	—
	CH127	97.18	0.83	0.07	0.02	0.65	1.11	0.991	−32.1	−26.8	−27.0	−163	−161	−123
	CH137	93.03	3.77	0.81	0.34	0.55	1.23	0.950	−34.5	−24.0	−21.4	−164	−125	—
	CG561	97.41	0.97	0.10	0.00	0.00	1.52	0.989	−32.9	−28.3	−27.8	−168	—	—
	CG561	93.69	3.96	0.56	0.22	0.37	1.04	0.952	−35.6	−22.7	−20.9	−176	−130	—
Zhongjiang-Huilong Structural Belt	CJ566	95.81	1.29	0.17	0.05	0.82	1.7	0.984	−33.7	−21.0	−19.8	—	—	—
	CJ566	95.86	1.75	0.23	0.09	0.36	1.60	0.979	−32.2	−22.1	—	−173	−110	—

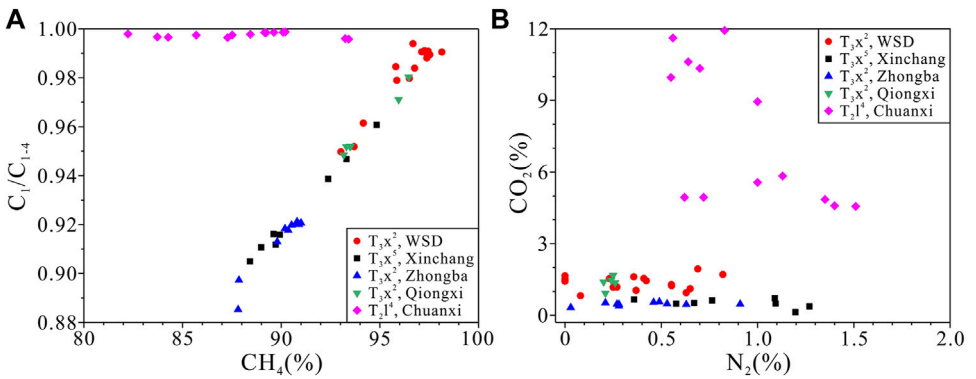

FIGURE 3 | The cross-plots of C_1/C_{1-4} versus CH_4% **(A)** and CO_2% versus N_2% **(B)**. The T_3x^2 gases of Zhongba and Qiongxi gas fields (Dai et al., 2012b), T_3x^5 gas from the Xinchang gas field (Wu et al., 2016), and T_2l^4 gas from the Chuanxi gas field (Wu et al., 2020b) are also plotted for comparative analysis and hereafter the same.

5 min, and then the temperature was programmed to 80°C at 8°C/min then heated to 260°C at 4°C/min where it was held for 10 min. Each gas sample was measured in triplicate, and the results were averaged. The measurement precision is estimated to be ±3‰ for δD with respect to VSMOW.

4 RESULTS

The chemical composition and stable isotopic compositions of the T_3x^2 tight gas from WSD are listed in **Table 1**. The previously published data of the T_3x^2 gases from Zhongba and Qiongxi gas fields (Dai et al., 2012b), T_3x^5 gas from the Xinchang gas field (Wu et al., 2016), and T_2l^4 gas from the Chuanxi gas field (Wu et al., 2020b) have also been collected for comparative analysis.

4.1 Main Components of Natural Gas

The T_3x^2 gas from WSD is mainly composed of CH_4, and the CH_4 content ranges from 93.03% to 98.14% with an average of 96.49%, whereas the heavy alkane (C_2–C_4) content ranges from 0.59% to 4.92% with an average of 1.72% (**Table 1**). The T_3x^2 gas from WSD is dry with the dryness coefficient (C_1/C_{1-4}) ranging from 0.950 to 0.994 (**Table 1**), and it displays a positive correlation between the CH_4 content and C_1/C_{1-4} ratio (**Figure 3A**), suggesting the effect of thermal maturity.

The non-hydrocarbon components of the T_3x^2 gas from WSD are predominantly CO_2 and N_2, with the contents ranging from 0.82% to 1.94% and from 0% to 0.82%, respectively (**Table 1**). The T_3x^2 gas is free of H_2S, and the correlation between CO_2 and N_2 contents is unobservable (**Figure 3B**).

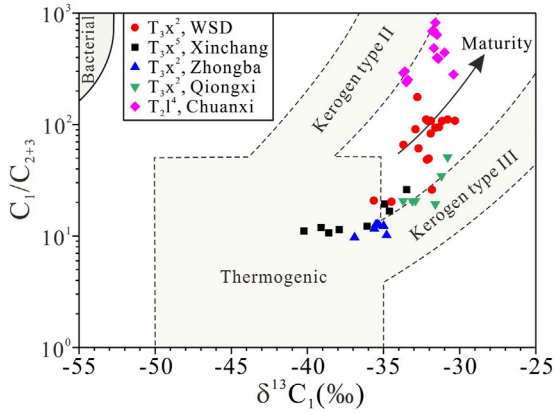

FIGURE 4 | The diagram of C_1/C_{2+3} versus $\delta^{13}C_1$ of the T_3x^2 gas from the Western Sichuan Depression (modified after Bernard et al., 1976).

4.2 Carbon Isotopes of Alkanes

The carbon isotopic value of CH_4 ($\delta^{13}C_1$) of T_3x^2 gas from WSD ranges from −35.6‰ to −30.3‰ with an average of −32.3‰, whereas the $\delta^{13}C_2$ value ranges from −29.1‰ to −21.0‰ with an average of −25.5‰ (**Table 1**). The gaseous alkanes mainly display positive carbon isotopic series (i.e., $\delta^{13}C_1 < \delta^{13}C_2 < \delta^{13}C_3$), with only a few samples possessing partial reversal between C_2H_6 and C_3H_8 ($\delta^{13}C_2 > \delta^{13}C_3$) (**Table 1**).

4.3 Hydrogen Isotopes of Alkanes

The hydrogen isotopic value of CH_4 (δD_1) of T_3x^2 gas from WSD ranges from −176‰ to −155‰ with an average of −163‰, whereas the δD_2 value ranges from −161‰ to −110‰ with an average of −138‰ (**Table 1**). The gas displays a positive hydrogen isotopic sequence between CH_4 and C_2H_6 (i.e., $\delta D_1 < \delta D_2$) (**Table 1**).

5 DISCUSSION

5.1 Genetic Types of Natural Gas

Biogenic gas consists of thermogenic gas and bacterial gas according to different mechanisms of gas generation, and the latter mostly has higher C_1/C_{2+3} ratios and lower $\delta^{13}C_1$ values (Bernard et al., 1976). The C_1/C_{2+3} ratios and $\delta^{13}C_1$ values of T_3x^2 gas from WSD range from 20.7 to 175.8 and from −35.6‰ to −30.3‰, respectively, suggesting the characteristics of thermogenic gas rather than bacterial gas (**Figure 4**). Thermogenic gas can be divided into coal-derived and oil-associated gases, which are generated by humic (kerogen type III) and sapropelic (kerogen type I/II) organic matters, respectively (Dai, 1992; Rooney et al., 1995; Liu et al., 2019). The Zhongba and Qiongxi T_3x^2 gases and Xinchang T_3x^5 gas follow the trend of natural gas from type III kerogen, suggesting the typical characteristics of coal-derived gas, whereas the Chuanxi T_2l^4 gas shares similar characteristics with natural gas from type II kerogen in the modified Bernard diagram (**Figure 4**). The T_3x^2 gas from WSD is mainly plotted between these two types of natural gas in the diagram (**Figure 4**), suggesting the characteristics of mixing gas, and it seems unlikely to be derived from single-type kerogen.

Coal-derived and oil-associated gases have different evolution trends in the correlation diagram between $\delta^{13}C_2$ and $\delta^{13}C_1$ values (Rooney et al., 1995), and oil-associated gas displays more negative $\delta^{13}C_2$ values than coal-derived gas under similar $\delta^{13}C_1$ values (**Figure 5A**). The Chuanxi T_2l^4 gas mainly follows the trend of oil-associated gas from type II kerogen in the Delaware/Val Verde Basin, whereas the Zhongba and Qiongxi T_3x^2 gases and Xinchang T_3x^5 gas follow the trend of coal-derived gas from type III kerogen in Niger Delta (**Figure 5A**). Several T_3x^2 gas samples from WSD are consistent with the coal-derived gas from type III kerogen in the diagram of $\delta^{13}C_2$ versus $\delta^{13}C_1$ values, whereas the other gas samples display the characteristics of oil-associated or mixing gas (**Figure 5A**), suggesting the complex features of the T_3x^2 gas.

The $\delta^{13}C_2$ and $\delta^{13}C_3$ values were considered to inherit the carbon isotopic compositions of original organic matter and thus could be used to identify the coal-derived and oil-associated gases (Dai et al., 2005). The geochemical statistics of natural gas in China indicated that the $\delta^{13}C_2$ values of coal-derived and oil-associated gases were commonly higher than −27.5‰ and lower than −29‰, respectively, whereas the $\delta^{13}C_3$ values were higher than −25.5‰ and lower than −27.0‰, respectively (Dai, 1999). The Zhongba and Qiongxi T_3x^2 gases and Xinchang T_3x^5 gas have consistent $\delta^{13}C_2$ and $\delta^{13}C_3$ values with typical coal-derived gas, whereas the only two T_2l^4 gas samples from the Chuanxi gas field display consistent $\delta^{13}C_2$ and $\delta^{13}C_3$ values with typical oil-associated gas (**Figure 5B**). Five gas samples in T_3x^2 reservoirs from WSD with relatively high $\delta^{13}C_2$ and $\delta^{13}C_3$ values display the characteristics of coal-derived gas, whereas the other gas samples are plotted in the transitional zone between oil-associated and coal-derived gas in **Figure 5B**, suggesting the characteristics of mixing gases.

Since the δD_1 values are associated with the types and thermal maturity of organic matter and water salinity (Liu et al., 2008; Schoell, 1980; Stahl, 1977), oil-associated gas and coal-derived gas generally follow different maturity trends in the correlation diagram between δD_1 and $\delta^{13}C_2$ values (**Figure 6**) (Wang et al., 2015). The Chuanxi T_2l^4 gas displays the characteristics of oil-associated gas with δD_1 values higher than −160‰, whereas the Zhongba and Qiongxi T_3x^2 gases and Xinchang T_3x^5 gas follow the trend of coal-derived gas in **Figure 6**. A positive correlation between δD_1 and $\delta^{13}C_2$ values is unobservable for the T_3x^2 gas from WSD, and most gas samples display the characteristics of mixing gas between typical oil-associated and coal-derived gases, with only five gas samples showing the characteristics of coal-derived gas (**Figure 6**). These indicate that most of the T_3x^2 gas samples from WSD follow the mixing trend rather than the maturity trend. Therefore, a small amount of the T_3x^2 gas from WSD is typically coal-derived gas, whereas most of the gas samples have experienced mixing by oil-associated gas.

The partial reversal of alkane carbon isotopes has been widely studied in China, and it can be attributed to mixing of abiogenic and biogenic gases, mixing of coal-derived and oil-associated

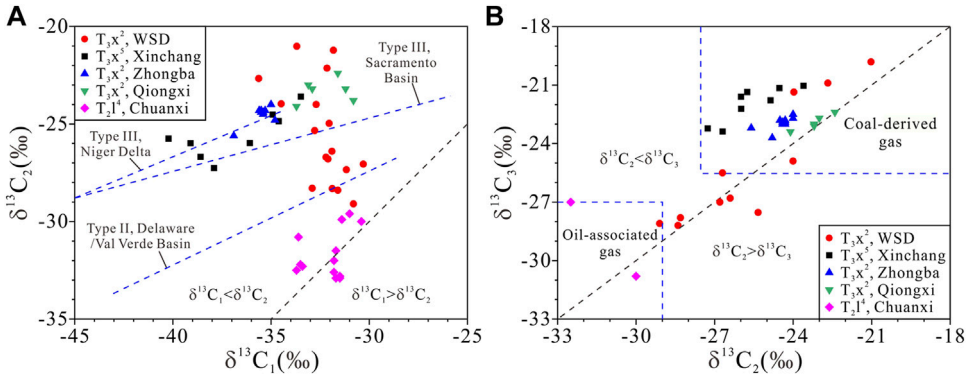

FIGURE 5 | The diagrams of $\delta^{13}C_2$ versus $\delta^{13}C_1$ **(A)** and $\delta^{13}C_3$ versus $\delta^{13}C_2$ **(B)**. The trends representing gases from Type III kerogen in Niger Delta and Type II kerogen in Delaware/Val Verde Basin **(A)** are after Rooney et al. (1995), and the trend for gas from Type III kerogen in Sacramento Basin **(A)** are after Jenden and Kaplan (1989). The ranges for coal-derived and oil-associated gases **(B)** are from Dai (1999).

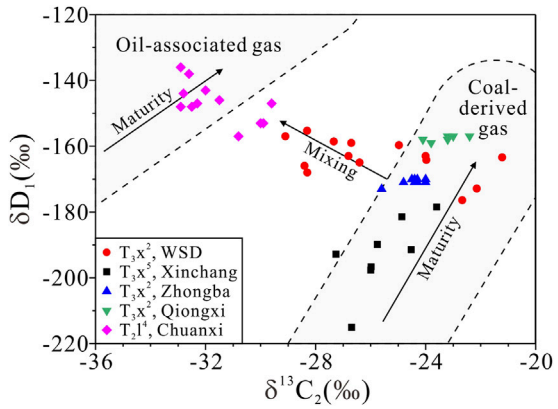

FIGURE 6 | Correlation diagram between δD_1 and $\delta^{13}C_2$ values of the T_3x^2 gas from the Western Sichuan Depression (modified after Wang et al., 2015).

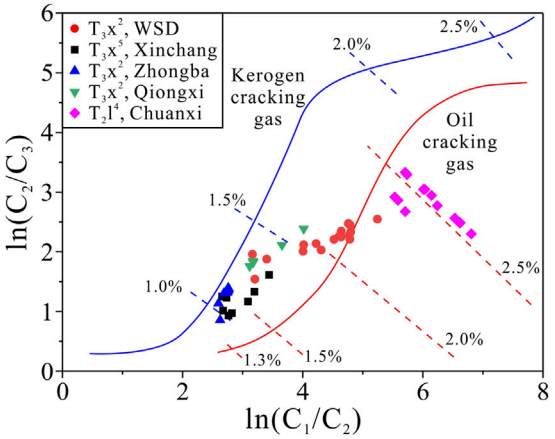

FIGURE 7 | The cross-plot of ln (C_2/C_3) versus ln (C_1/C_2) of the T_3x^2 gas from the Western Sichuan Depression (modified after Li et al., 2017).

gases, mixing of gases from the same types of source rocks with different maturity, or bacterial oxidation (Dai et al., 2004; Wu et al., 2014; Liu et al., 2019). Abiogenic gas or bacterial gas has not been found in WSD, and the mixing of abiogenic and biogenic gases or bacterial oxidation seems unlikely to happen. The mixing of coal-derived gas and oil-associated gas is demonstrated to be common in the T_3x^2 gas from WSD, and thus it is believed to be the main reason of partial $\delta^{13}C$ reversal between C_2H_6 and C_3H_8 ($\delta^{13}C_2 > \delta^{13}C_3$). The gas sample from Well JS1 displays a significantly heavier carbon isotope of C_2H_6 than that of C_3H_8 (**Table 1**). It is mainly caused by the extremely low $\delta^{13}C_3$ value (−27.5‰), which suggests the typical characteristics of oil-associated gas (**Figure 5B**). Therefore, the partial $\delta^{13}C$ reversal between C_2H_6 and C_3H_8 was attributed to mixing of coal-derived gas and oil-associated gas.

The coal-derived gas is commonly generated by humic organic matter (kerogen type III) through primary cracking of kerogen, whereas the oil-associated gas can be generated by both primary cracking of sapropelic kerogen (type II) and secondary cracking of oil, and the oil cracking gas accounts for nearly 80% of the total gas amount generated by sapropelic organic matter in the high-mature stage (Li et al., 2018). Natural gas in the marine strata of the Sichuan Basin is predominantly composed of oil-cracking gas (Hao et al., 2008; Liu et al., 2012; Liu et al., 2013; Liu et al., 2014). Theoretical and experimental studies indicate that kerogen cracking gas and oil cracking gas follow different evolution trends in the correlation diagram between ln (C_2/C_3) and ln (C_1/C_2) values (Prinzhofer and Huc, 1995; Li et al., 2017). The Chuanxi T_2l^4 oil-associated gas displays the characteristics of oil cracking gas (Wu et al., 2020b), whereas the coal-derived gas from the Zhongba and Qiongxi T_3x^2 and Xinchang T_3x^5 reservoirs primarily follows the trend of kerogen cracking gas (**Figure 7**). Three gas samples from the T_3x^2 reservoirs in WSD also follow the trend of kerogen cracking gas (**Figure 7**), and they have $\delta^{13}C_2$ values higher than −24.0‰ and display the characteristics of typical coal-derived gas in the correlation diagram between δD_1 and $\delta^{13}C_2$ values (**Figure 6**). Other gas samples from the T_3x^2 reservoirs in WSD are distributed closer

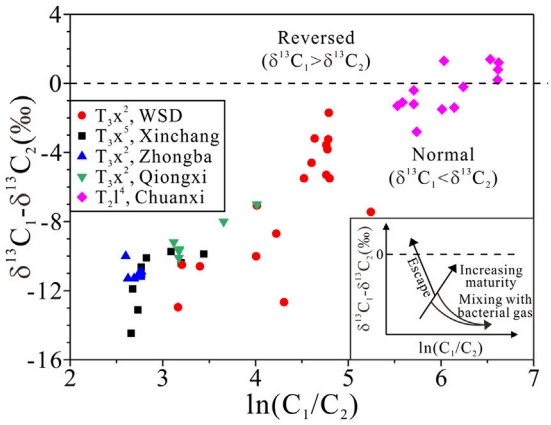

FIGURE 8 | The diagrams of $\delta^{13}C_1$-$\delta^{13}C_2$ versus ln (C_1/C_2) of the T_3x^2 gas from the Western Sichuan Depression (modified after Prinzhofer and Huc, 1995).

to the trend line of oil cracking gas in **Figure 7**; however, they are distinctly different from the oil cracking gas in the Chuanxi T_2l^4 reservoirs, which suggest that these T_3x^2 gas samples have experienced mixing by a significant amount of oil cracking gas. Therefore, the T_3x^2 tight gas from WSD are commonly mixed by oil cracking gas, except a few samples being typically coal-derived gas from kerogen cracking.

As indicated in **Figure 7**, the coal-derived gas in the T_3x^2 reservoirs from WSD seems to be mainly in the high-maturity stage with the maturity ranging from 1.3% to 1.7%, whereas the oil-associated gas reaches the over-mature stage with the maturity higher than 2.0%. The variance of the maturity may be attributed to the regional difference of potential source rocks, which was caused by different burial history and depth.

5.2 Gas—Source Correlation

5.2.1 Geochemical Comparison With the Chuanxi T_2l^4 Gas

The Chuanxi T_2l^4 gas is typical dry gas with the dryness coefficient (0.996–0.999) higher than the T_3x^2 gas from WSD (**Figure 3A**). The T_2l^4 gas is a sour gas with the H_2S content ranging from 0.59% to 4.90% (Wu et al., 2020b), and its CO_2 content (4.59%–15.25%) is apparently higher than the T_3x^2 gas from WSD (**Figure 3B**). These two gases share similar distribution ranges of $\delta^{13}C_1$ values; however, the Chuanxi T_2l^4 gas has higher C_1/C_{2+3} ratios (240–820) and thus the characteristics of oil-associated gas in the modified Bernard diagram (**Figure 4**), whereas the T_3x^2 gas from WSD displays the characteristics of mixing gas (**Figure 4**). The Chuanxi T_2l^4 gas has more negative $\delta^{13}C_2$ values (−32.9‰ to −29.6‰) and less negative δD_1 values (−157‰ to −136‰), resulting in different distribution characteristics with the T_3x^2 gas from WSD in **Figure 5A** and **Figure 6**. The larger ln (C_2/C_3), ln (C_1/C_2), and $\delta^{13}C_1$-$\delta^{13}C_2$ values of the Chuanxi T_2l^4 gas suggest higher thermal maturity than the T_3x^2 gas from WSD (**Figure 7**, **Figure 8**).

The Chuanxi T_2l^4 gas was demonstrated as typical oil-associated gas and derived mainly from the underlying Upper Permian source rocks (Wu et al., 2020b), and the gas pools were commonly distributed along the deep fault which directly or indirectly connected the reservoirs and the Permian strata (Wu et al., 2020a). The T_3x^2 gas from WSD is apparently different from typical oil-associated gas (**Figure 4**, **Figure 5A**, **Figure 6**), and the thermal maturity is significantly lower than the Chuanxi T_2l^4 gas (**Figure 7**, **Figure 8**). Therefore, the T_3x^2 gas from WSD displays few affinities with the Upper Permian source rocks.

5.2.2 Geochemical Comparison With the Xinchang T_3x^5 Gas

The Xinchang T_3x^5 gas is mainly wet gas with the dryness coefficient ranging from 0.905 to 0.961 (Wu et al., 2016), which is principally lower than that of the T_3x^2 gas from WSD (**Figure 3A**). The CO_2 content ranges from 0.13% to 0.70% and is also lower than that of the T_3x^2 gas from WSD (**Figure 3B**). The $\delta^{13}C_1$ and C_1/C_{2+3} values of the Xinchang T_3x^5 gas, ranging from −40.2‰ to −33.5‰ and from 10.7 to 26.0, respectively, are generally lower than the corresponding values of the T_3x^2 gas from WSD (**Figure 4**). This suggests a relatively lower thermal maturity of the Xinchang T_3x^5 gas. In the modified Bernard diagram (**Figure 4**), the Xinchang T_3x^5 gas follows the typical characteristics of coal-derived gas from type III kerogen, and it is different from the transitional or mixing characteristics of the T_3x^2 gas from WSD. The $\delta^{13}C_2$ and $\delta^{13}C_3$ values of the Xinchang T_3x^5 gas, concentrating from −27.3‰ to −23.6‰ and from −23.4‰ to −21.0‰, respectively, display differences with the wide distribution ranges of corresponding values of T_3x^2 gas from WSD (**Figure 5**). The Xinchang T_3x^5 gas has the δD_1 value ranging from −215‰ to −179‰, which is obviously lower than the T_3x^2 gas from WSD (**Figure 6**). Moreover, the relatively lower ln (C_2/C_3) and ln (C_1/C_2) values of the Xinchang T_3x^5 gas indicate its lower thermal maturity than the T_3x^2 gas from WSD (**Figure 7**, **Figure 8**).

The Xinchang T_3x^5 gas was demonstrated as typical coal-derived gas and mainly generated by the T_3x^5 source rocks (Wu et al., 2016). The T_3x^2 gas from WSD displays certain differences with typical coal-derived gas (**Figures 4**,**5**, **6**), and the thermal maturity is apparently higher than the Xinchang T_3x^5 gas (**Figures 7**, **8**). Consequently, the T_3x^2 gas from WSD displays few affinities with the T_3x^5 source rocks, and it is considered to be derived from source rocks with higher thermal maturity.

5.2.3 Geochemical Comparison With the Zhongba and Qiongxi T_3x^2 Gases

The Qiongxi T_3x^2 gas is mainly dry gas with the dryness coefficients between 0.948 and 0.980, whereas the Zhongba T_3x^2 gas is typical wet gas with the dryness coefficient ranging between 0.885 and 0.921 (Dai et al., 2012b). They are both apparently lower than the coefficient of the T_3x^2 gas from WSD (**Figure 3A**). The Qiongxi T_3x^2 gas has consistent CO_2 content (from 0.92% to 1.67%) with the T_3x^2 gas from WSD, whereas the Zhongba T_3x^2 gas displays an obviously lower CO_2 content (from 0.32% to 0.56%) than the T_3x^2 gas from WSD (**Figure 3B**).

Compared with the T_3x^2 gas from WSD, the Qiongxi T_3x^2 gas displays similar $\delta^{13}C_1$ values (ranging from −33.7‰ to −30.8‰) and overall lower C_1/C_{2+3} ratios (from 19.3 to 50.8), whereas the Zhongba T_3x^2 gas has apparently lower $\delta^{13}C_1$ values (ranging from −36.9‰ to −34.8‰) and C_1/C_{2+3} ratios (from 9.7 to 12.7)

(**Figure 4**). There are two gases that show the characteristics of coal-derived gas in the modified Bernard diagram (**Figure 4**). Their $\delta^{13}C_2$ values are distributed in the narrow ranges from −24.1‰ to −22.4‰ and from −25.6‰ to −24.0‰, respectively, whereas the δD_1 values range from −159‰ to −157‰ and from −173‰ to −170‰, respectively, with $\delta^{13}C_3$ values higher than −24‰ (Dai et al., 2012b). They also follow the typical characteristics of coal-derived gas in **Figure 5A,B** and **Figure 6** and displays certain differences with the T_3x^2 gas from WSD.

The Qiongxi and Zhongba T_3x^2 gases were demonstrated to be self-generated and self-accumulated in T_3x, i.e., they were mainly derived from the T_3x^1 coal–measure source rocks with assistance of T_3x^2 coal–measure source rocks (Zhu et al., 2011; Dai et al., 2012b; Liao et al., 2014). Affected by different largest burial depths, the present thermal maturity of T_3x^1 in the Zhongba gas field is slightly lower than that in the Qiongxi gas field and WSD (Jiang et al., 2012). This is consistent with the maturity difference indicated by the ln (C_2/C_3), ln (C_1/C_2), and $\delta^{13}C_1$-$\delta^{13}C_2$ values of the T_3x^2 gases in these areas (**Figures 7**, **8**). Therefore, the geochemical characteristics of the T_3x^2 gas from WSD match the thermal maturity of the *in-situ* T_3x^1 and T_3x^2 source rocks.

5.2.4 Source of the T_3x^2 Gas From WSD

The above geochemical analysis and genetic identification of natural gas indicate that the T_3x^2 gas from WSD is mainly coal-derived gas assisted by oil-associated gas, rather than typical coal-derived or oil-associated gas. Therefore, it is unreliable to calculate the thermal maturity by $\delta^{13}C_1$ values based on the $\delta^{13}C_1$-R_O empirical equations for typical coal-derived or oil-associated gas. According to the thermal maturity comparison indicated by geochemical characteristics of natural gas from different strata, the T_3x^2 gas from WSD displays apparently higher maturity than the overlying Xinchang T_3x^5 gas and lower maturity than the underlying Chuanxi T_2l^4 gas (**Figures 7**, **8**). The T_3x^2 gas from WSD is inferred to have consistent maturity with the T_3x^1 and T_3x^2 source rocks.

The T_3x source rocks in the Sichuan Basin were mainly developed in T_3x^1, T_3x^3, and T_3x^5, and a small amount of argillaceous source rocks was developed in T_3x^2, T_3x^4, and T_3x^6 (Dai et al., 2009; Wang et al., 2010; Cai and Yang, 2011; Dai et al., 2012b). T_3x^1 is commonly divided into Xiaotangzi (T_3t) and underlying Ma'antang (T_3m) formations, in which T_3t consists of sandstone interbedded with mudstone and siltstone, and T_3m is composed of silty mudstone at the top and grey limestone at the bottom (**Figure 2**). The kerogen-type indexes of T_3t and T_3m mudstone are less than 0 and consistent with those of the T_3x^2 mudstone, displaying the characteristics of typical type III kerogen, whereas the indexes of the T_3m limestone range from 23.75 to 50.5, displaying the characteristics of type II kerogen (Wang et al., 2010; Cai and Yang, 2011). The T_3m limestone from some areas in WSD displays certain hydrocarbon potential with the TOC contents higher than 0.5% (Yang et al., 2012). Therefore, among the T_3x^2 tight gas from WSD the coal-derived gas is generated mainly by the T_3t and T_3m mudstone with assistance of T_3x^2 mudstone, whereas the oil-associated gas is derived from the T_3m limestone.

6 CONCLUSION

The tight gas in Member two of the Upper Triassic Xujiahe Formation in the WSD of the Sichuan Basin is mainly composed of CH_4, with the CH_4 content ranging from 93.03% to 98.14%. The dryness coefficient of the tight gas is 0.950–0.994 and positively correlated with the CH_4 content. The gaseous alkanes display positive carbon isotopic series, with the $\delta^{13}C_1$ and $\delta^{13}C_2$ values ranging from −35.6‰ to −30.3‰ and from −29.1‰ to −21.0‰, respectively, and the δD_1 values range from −176‰ to −155‰.

According to the genetic identification based on the carbon and hydrogen isotopic compositions, a small amount of the tight gas is typically coal-derived gas, whereas most of the tight-gas samples have experienced mixing by oil-associated gas. Geochemical comparisons indicate that the tight gas displays distinct differences with the typical oil-associated and coal-derived gases in adjacent gas fields. Among the tight gas in Member two of the Xujiahe Formation from the WSD, the coal-derived gas is generated mainly by the humic mudstone in the Upper Triassic Ma'antang and Xiaotangzi formations, with assistance of the humic mudstone in Member two of the Xujiahe Formation, whereas the oil-associated gas is derived from the sapropelic limestone in the Ma'antang Formation.

DATA AVAILABILITY STATEMENT

The original contributions presented in the study are included in the article/Supplementary Material; further inquiries can be directed to the corresponding author.

AUTHOR CONTRIBUTIONS

XW: conceptulization, data curation, writing. QL: conceptulization, writing. YC: data curation, methodology. JY: methodology, investigation. HZ: sample collection, investigation. HL: investigation.

FUNDING

This work was funded by the National Natural Science Foundation of China (Grant Nos. 42172149, 41872122, U20B6001, and 42141021) and Strategic Priority Research Program of the Chinese Academy of Sciences (Class A) (Grant Nos. XDA14010402 and XDA14010404).

ACKNOWLEDGMENTS

The authors appreciate Jinxing Dai, Academician of Chinese Academy of Sciences, for the long-standing guidance of the relevant studies. We also appreciate QL for the valuable discussion and inspiration. The SINOPEC Southwest Branch Company and Key Laboratory for Hydrocarbon Accumulation Mechanism are acknowledged for the assistance on sample collection and geochemical analyses, respectively.

REFERENCES

Bernard, B. B., Brooks, J. M., and Sackett, W. M. (1976). Natural Gas Seepage in the Gulf of Mexico. *Earth Planet. Sci. Lett.* 31, 48–54. doi:10.1016/0012-821x(76)90095-9

Cai, X., and Yang, K. (2011). *Tight sandstone Gas Pools in the Xujiahe Formation, Western Sichuan Depression*. Beijing: Petroleum Industry Press.

Dai, J. (2016). *Giant Coal-Derived Gas Fields and Their Gas Sources in China*. Beijing: Science Press.

Dai, J. (1992). Identification and Distinction of Various Alkane Gases. *Sci. China (Series B)* 35, 1246–1257.

Dai, J., Ni, Y., Hu, G., Huang, S., Liao, F., Yu, C., et al. (2014). Stable Carbon and Hydrogen Isotopes of Gases from the Large Tight Gas fields in China. *Sci. China Earth Sci.* 57, 88–103. doi:10.1007/s11430-013-4701-7

Dai, J., Ni, Y., Qin, S., Huang, S., Peng, W., and Han, W. (2018). Geochemical Characteristics of Ultra-deep Natural Gas in the Sichuan Basin, SW China. *Pet. Exploration Dev.* 45, 619–628. doi:10.1016/s1876-3804(18)30067-3

Dai, J., Ni, Y., and Wu, X. (2012a). Tight Gas in China and its Significance in Exploration and Exploitation. *Pet. Exploration Dev.* 39, 277–284. doi:10.1016/s1876-3804(12)60043-3

Dai, J., Ni, Y., and Zou, C. (2012b). Stable Carbon and Hydrogen Isotopes of Natural Gases Sourced from the Xujiahe Formation in the Sichuan Basin, China. *Org. Geochem.* 43, 103–111. doi:10.1016/j.orggeochem.2011.10.006

Dai, J., Ni, Y., Zou, C., Tao, S., Hu, G., Hu, A., et al. (2009). Stable Carbon Isotopes of Alkane Gases from the Xujiahe Coal Measures and Implication for Gas-Source Correlation in the Sichuan Basin, SW China. *Org. Geochem.* 40, 638–646. doi:10.1016/j.orggeochem.2009.01.012

Dai, J., Qin, S., Tao, S., Zhu, G., and Mi, J. (2005). Development Trends of Natural Gas Industry and the Significant Progress on Natural Gas Geological Theories in China. *Nat. Gas Geosci.* 16, 127–142. doi:10.11764/j.issn.1672-1926.2005.02.127

Dai, J. (1999). Significant Advancement in Research on Coal-Formed Gas in China. *Pet. Exploration Dev.* 26, 1–10. cnki:sun:skyk.0.1999-03-000.

Dai, J., Xia, X., Qin, S., and Zhao, J. (2004). Origins of Partially Reversed Alkane δ 13 C Values for Biogenic Gases in China. *Org. Geochem.* 35, 405–411. doi:10.1016/j.orggeochem.2004.01.006

Hao, F., Guo, T., Zhu, Y., Cai, X., Zou, H., and Li, P. (2008). Evidence for Multiple Stages of Oil Cracking and Thermochemical Sulfate Reduction in the Puguang Gas Field, Sichuan Basin, China. *Bulletin* 92, 611–637. doi:10.1306/01210807090

Jenden, P. D., and Kaplan, I. R. (1989). Origin of Natural Gas in Sacramento Basin, California. *AAPG Bull.* 73, 431–453. doi:10.1306/44b49fc9-170a-11d7-8645000102c1865d

Jiang, X., Zeng, H., Zhu, J., and Cao, Q. (2012). Dynamic Evolution Simulation of the Upper Triassic Source Rocks in central Part of Western Sichuan Depression. *Oil Gas Geology.* 33, 545–551. doi:10.11743/ogg20120408

Li, J., Li, Z., Wang, X., Wang, D., Xie, Z., Li, J., et al. (2017). New Indexes and Charts for Genesis Identification of Multiple Natural Gases. *Pet. Exploration Dev.* 44, 535–543. doi:10.1016/s1876-3804(17)30062-9

Li, J., Ma, W., Wang, Y., Wang, D., Xie, Z., Li, Z., et al. (2018). Modeling of the Whole Hydrocarbon-Generating Process of Sapropelic Source Rock. *Pet. Exploration Dev.* 45, 461–471. doi:10.1016/s1876-3804(18)30051-x

Liao, F., Yu, C., Wu, W., and Liu, D. (2014). Stable Carbon and Hydrogen Isotopes of Natural Gas from the Zhongba Gasfield in the Sichuan Basin and Implication for Gas-Source Correlation. *Nat. Gas Geosci.* 25, 79–86. doi:10.11764/j.issn.1672-1926.2014.01.0079

Liu, Q., Dai, J., Li, J., and Zhou, Q. (2008). Hydrogen Isotope Composition of Natural Gases from the Tarim Basin and its Indication of Depositional Environments of the Source Rocks. *Sci. China Ser. D-earth Sci.* 51, 300–311. doi:10.1007/s11430-008-0006-7

Liu, Q., Jin, Z., Li, J., Hu, A., and Bi, C. (2012). Origin of marine Sour Natural Gas and Gas-Filling Model for the Wolonghe Gas Field, Sichuan Basin, China. *J. Asian Earth Sci.* 58, 24–37. doi:10.1016/j.jseaes.2012.07.007

Liu, Q., Wu, X., Wang, X., Jin, Z., Zhu, D., Meng, Q., et al. (2019). Carbon and Hydrogen Isotopes of Methane, Ethane, and Propane: A Review of Genetic Identification of Natural Gas. *Earth-Science Rev.* 190, 247–272. doi:10.1016/j.earscirev.2018.11.017

Liu, Q. Y., Worden, R. H., Jin, Z. J., Liu, W. H., Li, J., Gao, B., et al. (2014). Thermochemical Sulphate Reduction (TSR) versus Maturation and Their Effects on Hydrogen Stable Isotopes of Very Dry Alkane Gases. *Geochimica et Cosmochimica Acta* 137, 208–220. doi:10.1016/j.gca.2014.03.013

Liu, Q. Y., Worden, R. H., Jin, Z. J., Liu, W. H., Li, J., Gao, B., et al. (2013). TSR versus Non-TSR Processes and Their Impact on Gas Geochemistry and Carbon Stable Isotopes in Carboniferous, Permian and Lower Triassic marine Carbonate Gas Reservoirs in the Eastern Sichuan Basin, China. *Geochimica et Cosmochimica Acta* 100, 96–115. doi:10.1016/j.gca.2012.09.039

Liu, Q., Zhu, D., Jin, Z., Liu, C., Zhang, D., and He, Z. (2016). Coupled Alteration of Hydrothermal Fluids and thermal Sulfate Reduction (TSR) in Ancient Dolomite Reservoirs - an Example from Sinian Dengying Formation in Sichuan Basin, Southern China. *Precambrian Res.* 285, 39–57. doi:10.1016/j.precamres.2016.09.006

Ni, Y., Dai, J., Tao, S., Wu, X., Liao, F., Wu, W., et al. (2014a). Helium Signatures of Gases from the Sichuan Basin, China. *Org. Geochem.* 74, 33–43. doi:10.1016/j.orggeochem.2014.03.007

Ni, Y., Liao, F., Dai, J., Zou, C., Wu, X., Zhang, D., et al. (2014b). Studies on Gas Origin and Gas Source Correlation Using Stable Carbon Isotopes - A Case Study of the Giant Gas Fields in the Sichuan Basin, China. *Energy Exploration & Exploitation* 32, 41–74. doi:10.1260/0144-5987.32.1.41

Prinzhofer, A. A., and Huc, A. Y. (1995). Genetic and post-genetic Molecular and Isotopic Fractionations in Natural Gases. *Chem. Geology.* 126, 281–290. doi:10.1016/0009-2541(95)00123-9

Rooney, M. A., Claypool, G. E., and Moses Chung, H. (1995). Modeling Thermogenic Gas Generation Using Carbon Isotope Ratios of Natural Gas Hydrocarbons. *Chem. Geology.* 126, 219–232. doi:10.1016/0009-2541(95)00119-0

Schoell, M. (1980). The Hydrogen and Carbon Isotopic Composition of Methane from Natural Gases of Various Origins. *Geochimica et Cosmochimica Acta* 44, 649–661. doi:10.1016/0016-7037(80)90155-6

Stahl, W. J. (1977). Carbon and Nitrogen Isotopes in Hydrocarbon Research and Exploration. *Chem. Geology.* 20, 121–149. doi:10.1016/0009-2541(77)90041-9

Wang, D., Zeng, H., and Wang, J. (2010). Evaluation on Upper Triassic Hydrocarbon Source Rocks of Western Sichuan Depression, Sichuan Basin. *Pet. Geology. Exp.* 32, 192–195. doi:10.11781/sysydz201002192

Wang, X., Liu, W., Shi, B., Zhang, Z., Xu, Y., and Zheng, J. (2015). Hydrogen Isotope Characteristics of Thermogenic Methane in Chinese Sedimentary Basins. *Org. Geochem.* 83-84, 178–189. doi:10.1016/j.orggeochem.2015.03.010

Wu, X., Chen, Y., Zhai, C., Zhou, X., Liu, W., Yang, J., et al. (2020a). Gas Source and Exploration Direction of the Middle Triassic Leikoupo Formation in the Sichuan Basin, China. *J. Nat. Gas Geosci.* 5, 317–326. doi:10.1016/j.jnggs.2020.10.001

Wu, X., Liu, Q., Chen, Y., Zhai, C., Ni, C., and Yang, J. (2020b). Constraints of Molecular and Stable Isotopic Compositions on the Origin of Natural Gas from Middle Triassic Reservoirs in the Chuanxi Large Gas Field, Sichuan Basin, SW China. *J. Asian Earth Sci.* 204, 104589. doi:10.1016/j.jseaes.2020.104589

Wu, X., Liu, Q., Liu, G., and Ni, C. (2019). Genetic Types of Natural Gas and Gas-Source Correlation in Different Strata of the Yuanba Gas Field, Sichuan Basin, SW China. *J. Asian Earth Sci.* 181, 103906. doi:10.1016/j.jseaes.2019.103906

Wu, X., Liu, Q., Liu, G., Wang, P., Li, H., Meng, Q., et al. (2017). Geochemical Characteristics and Genetic Types of Natural Gas in the Xinchang Gas Field, Sichuan Basin, SW China. *Acta Geologica Sinica - English Edition* 91, 2200–2213. doi:10.1111/1755-6724.13458

Wu, X., Liu, Q., Tao, X., and Hu, G. (2014). Geochemical Characteristics of Natural from Halahatang Sag in the Tarim Basin. *Geochimica* 43, 477–488. doi:10.19700/j.0379-1726.2014.05.006

Wu, X., Wang, P., Liu, Q., Li, H., Chen, Y., Zeng, H., et al. (2016). The Source of Natural Gas Reservoired in the 5th Member of the Upper Triassic Xujiahe Formation in Xinchang Gasfield, the Western Sichuan Depression and its Implication. *Nat. Gas Geosci.* 27, 1409–1418. doi:10.11764/j.issn.1672-1926.2016.08.1409

Yang, J., Zhang, M., and Chen, X. (2012). Identification of Xu1 Member as Main Source Rock in Upper Triassic from West Sichuan Depression. *J. Yangtze Univ. (Natural Sci. Edition)* 9 (12), 41–43. doi:10.3969/j.issn.1673-1409(N).2012.12.013

Zhang, D. (2021). Development prospect of Natural Gas Industry in the Sichuan Basin in the Next Decade. *Nat. Gas Industry* 41, 34–45. doi:10.3787/j.issn.1000-0976.2021.08.004

Zhu, G., Zhang, S., Huang, H., Liang, Y., Meng, S., and Li, Y. (2011). Gas Genetic Type and Origin of Hydrogen Sulfide in the Zhongba Gas Field of the Western Sichuan Basin, China. *Appl. Geochem.* 26, 1261–1273. doi:10.1016/j.apgeochem.2011.04.016

Conflict of Interest: HL was employed by Exploration and Production Research Institute, Southwest Branch Company.

The remaining authors declare that the research was conducted in the absence of any commercial or financial relationships that could be construed as a potential conflict of interest.

Publisher's Note: All claims expressed in this article are solely those of the authors and do not necessarily represent those of their affiliated organizations, or those of the publisher, the editors, and the reviewers. Any product that may be evaluated in this article, or claim that may be made by its manufacturer, is not guaranteed or endorsed by the publisher.

Copyright © 2022 Wu, Liu, Chen, Yang, Zeng and Li. This is an open-access article distributed under the terms of the Creative Commons Attribution License (CC BY). The use, distribution or reproduction in other forums is permitted, provided the original author(s) and the copyright owner(s) are credited and that the original publication in this journal is cited, in accordance with accepted academic practice. No use, distribution or reproduction is permitted which does not comply with these terms.